Korean J. Chem. Eng., **30**(6), 1326-1334 (2013)
DOI: 10.1007/s11814-013-0030-y

Prediction of bed pressure drop and top packed bed formation in gas-liquid-solid semi-fluidized bed with irregular homogeneous binary mixtures

Deepak Kumar Samal†, Yashobanta Kumar Mohanty, and Gopendra Kishore Roy

Department of Chemical Engineering, Gandhi Institute of Engineering and Technology (GIET), Gunupur, Rayagada, Odisha-765022, India
(*Received 21 November 2012 • accepted 24 February 2013*)

Abstract−We studied the hydrodynamics of a gas-liquid-solid semi-fluidized bed relating to packed bed formation and bed pressure drop with irregular homogeneous binary mixtures in a 0.05 m internal diameter Perspex column, with water and air (secondary) as fluidizing medium at constant static bed height of 0.08 m. A homogeneous binary mixture has been taken for easy formation of a semi-fluidized bed. Air is supplied centrally below the bottom grid in radial direction with a special design air sparger after the bed is first fluidized by the liquid. Experimental parameters studied included superficial gas and liquid velocities, average particle size and density and the bed expansion ratio. Empirical and semi-empirical models were developed. The calculated values from predicted models were compared with the experimental values and fairly good agreement was obtained.

Key words: Gas-liquid-solid Semi-fluidization, Irregular Homogeneous Binary Mixtures, Bed Pressure Drop, Top Packed Bed Formation, Dimensional and Statistical Analyses

INTRODUCTION

Three-phase semi-fluidization is a gas-liquid-solid contacting operation that has great importance when the gas phase has a prominent role, especially for fermentation and waste water treatment, where micro-organisms and solid catalysts are involved. A semi-fluidized bed is obtained by increasing the fluid velocity beyond the minimum fluidization condition, and thereafter arresting the movement of the solid particles with a restraint fixed at a suitable height towards the top of the conduit. The top packed bed can be formed by increasing fluid velocity alone in the case of two-phase semi-fluidization or by increasing the velocity of one of the fluids or both in case of three-phase semi-fluidization. This results in the formation of a packed bed below the top restraint. The velocity at which the first particle of solid touches the top restraint is called the minimum semi-fluidization velocity (U_{osf}) (as the case). Similarly, when all the solid particles in the column form a packed bed below the top restraint, the corresponding fluid velocity is called the maximum semi-fluidization velocity (U_{msf}), which is generally obtained by extrapolation of H_{pa}/H_s vs G plot to H_{pa}/H_s to 1, as in most of the cases total transfer of bed materials to the top may not be feasible due to experimental constraints. The above velocities are defined generally with respect to the continuous phase in case of a three-phase semi-fluidization.

Development and advantages of the semi-fluidized bed relating to studies on hydrodynamics and mass transfer started in 1959 [1]. The single size particle hydrodynamic study in solid-liquid system was highlighted by Fan and Wen in 1961 [2]. Investigations relating to various aspects of a semi-fluidized bed involving different systems are available in literature. Considerable work on the hydrodynamic studies of a semi-fluidized bed has been reported [3-6]. Murthy and Roy presented a review article on semi-fluidization [7]. Most of the above studies relate to a single component, excepting a few relating to binary homogeneous and heterogeneous mixtures [4,5,8,9]. Investigations relating to three-phase semi-fluidization of a single component are limited [10-14], while that for homogeneous binary mixtures is almost absent, though three-phase fluidization with binary mixture particle has been studied [15]. Various applications in different fields have been reported in the literature where semi-fluidization plays an important role [16-20].

Our objective was to study a few aspects of hydrodynamics of gas-liquid-solid semi-fluidization, namely, bed pressure drop and height of top packed bed formation in a semi-fluidized bed using homogeneous binary mixtures of irregular particles of five different materials. Investigations were conducted in a 0.05 m internal diameter Perspex column with an initial static bed height of 0.08 m. The effect of the system parameters studied includes superficial liquid velocity (U_{sfl}), superficial gas velocity (U_{sfg}), average particle diameter (d_{pav}, based on wt%), particle density (ρ_{sav}) and bed expansion ratio (R). The bed expansion ratio (R) is defined as the height of top restraint from the bottom grid to the initial static bed height of solid particles, which is also an indication of the top restraint position. The experimental data were correlated with the system parameters by two different approaches: dimensional and statistical analyses.

EXPERIMENTAL SETUP AND TECHNIQUE

Schematic and pictorial representations of the experimental setup are shown in Fig. 1. The experimental semi-fluidized bed consists of a fluidized bed assembly, a top restraint with fixture, and two U-tube manometers with carbon tetrachloride (for low pressure range) and mercury (for high pressure range) as the manometric fluids. The fluidized bed assembly consists of a fluidizer, a liquid distribu-

†To whom correspondence should be addressed.
E-mail: deepakkumarsamal@rediffmail.com

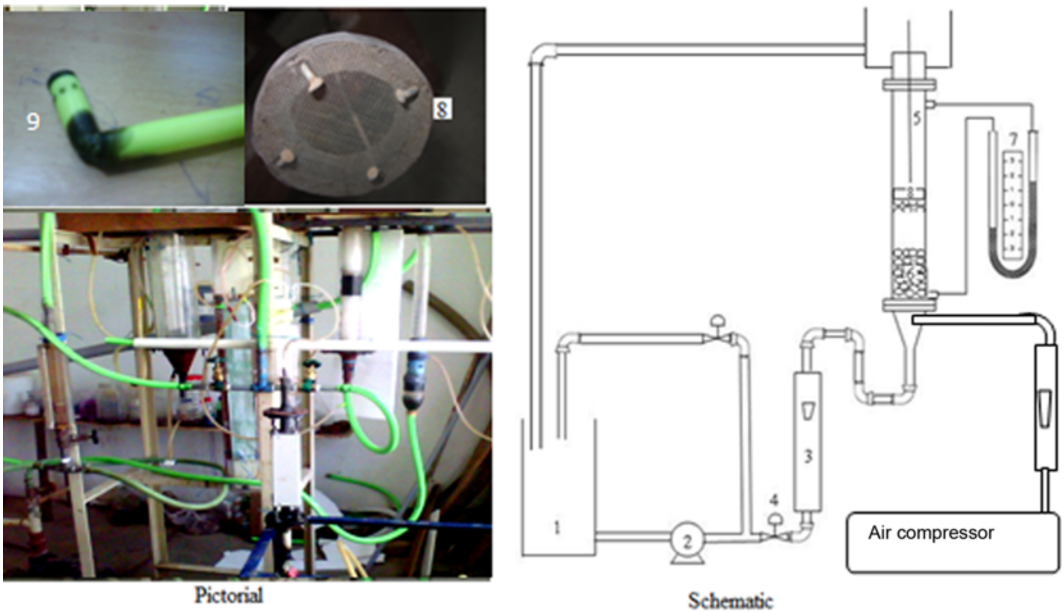

Fig. 1. Experimental setup.

1. Liquid tank	3. Rotameter	5. Semi-fluidized column	7. U-tube manometer	9. Air sparger
2. Liquid pump	4. Control valve	6. Semi-fluidized bed	8. Restraint	

tor, a disengagement and recirculation facility, an air compressor, a pump (2HP), a liquid storage tank (250 lit.) and a set of calibrated liquid rotameters (max. 600LPH, 1080LPH, 2000LPH).

The fluidizer is a cylindrical Plexiglas column of 0.05 m internal diameter and 0.62 m height. For achieving uniform flow for the continuous phase in the column, the bottom conical section is filled with spherical ceramic pebbles of size 0.005 m diameter to which the air sparger is centrally fixed. The liquid inlet pipe of 0.0127 m in internal diameter is located centrally to the conical bottom. The higher cross-section end of the conical bottom is flanged with the fluidizer with a 40 mesh (BSS) screen as its bottom grid. The liquid disengagement section at the top of the column is a rectangular section of 0.3×0.3×0.2 m dimension, fixed with the column, which allows holdup of the liquid and the balance is circulated. Air is supplied to the bottom conical section with the help of an air sparger of diameter 0.005 m as shown in Fig. 1.

The top restraint is made from a Perspex sheet of 0.048 m outer diameter and 0.038 m inner diameter and is 10mm thick, containing a number of 0.002 m holes arranged in a square pitch. A 40 mesh (BSS) screen is attached to it and fixed with perforated iron tube as shown in Fig. 1. A rubber pipe of diameter 0.004 m is fixed on the outer circumference of the restraint for smooth movement of the restraint inside the column and also to not allow solid particles to go out of the bed along the wall of the column. A photographic view of the top restraint is presented in Fig. 1.

The scope of the experiment is presented in Table 1. In view of the fact that a semi-fluidized bed can operate without segregation only when homogeneous binary mixtures of solids are used with a particle size ratio less than 1.3 [19], a mixture of particle sizes of 0.001854 m (d_{p1}) and 0.0015405 m (d_{p2}) of different compositions

Table 1. Scope of the experiment

(A) Properties of bed material		(B) Binary mixture properties			
	Particle size ($d_p \times 10^3$, m)		Mixture	Composition (wt%)	Avg. particle size ($d_{pav} \times 10^3$ m)
d_{p1}	1.854		Mixture 1	50 : 50	1.6825
d_{p2}	1.5405		Mixture 2	60 : 40	1.7142
			Mixture 3	70 : 30	1.7471
			Mixture 4	80 : 20	1.7814
			Mixture 5	90 : 10	1.8169
(C) Materials					
Materials	Coal	Bauxite	Dolomite	Chromite	Iron ore
ρ_s, kg/m^3	1600	2100	2800	3300	4200
(D) Bed expansion ratio					
R	1.5	2.0	2.5	3.0	3.5

(wt%) was used in the present investigation. Accurately weighed amount of material was fed into the column, fluidized and de-fluidized slowly and adjusted for a specific reproducible initial static bed height of 0.08 m. Liquid was pumped to the fluidizer through a rotameter increasing the flow to the minimum fluidization condition. Thereafter, air metered through a rotameter was bubbled through the sparger and the three-phase semi-fluidized bed became operational. Temperature was maintained at 30±5 °C. To ensure steady state operation, at least five minutes was allowed before each reading after the onset of semi-fluidization .The readings of the manometers and the top packed bed heights for each liquid as well as gas flow rate were then noted. The procedure was repeated varying the superficial liquid and gas velocities, the average particle diameter and particle density and bed expansion ratio.

In this work, both dimensional and statistical analyses have been used to predict mathematical models for responses like dimensionless semi-fluidized bed pressure drop ($\Delta P_{sf}/\Delta P_{mf}$) and dimensionless top packed bed height (H_{pa}/H_s). In dimensional analysis, the following mathematical model is used for different responses,

$$\Delta P_{sf}/P_{mf}=K'(\rho_{sav}/\rho_l)^{k1}(D_c/d_{pav})^{k2}(U_{sfg}/U_{mf})^{k3}(U_{sfl}/U_{mf})^{k4}R^{k5} \quad (1)$$

$$H_{pa}/H_s=K''(\rho_{sav}/\rho_l)^{k6}(D_c/d_{pav})^{k7}(U_{sfg}/U_{mf})^{k8}(U_{sfl}/U_{mf})^{k9}R^{k10} \quad (2)$$

For statistical analysis, central composite design (CCD) has been used to develop correlations with five independent dimensionless variables--ρ_{sav}/ρ_l, D_c/d_{pav}, U_{sfg}/U_{mf}, U_{sfl}/U_{mf}, and R for two dependent dimensionless variables: the bed pressure drop ($\Delta P_{sf}/\Delta P_{mf}$) and the top packed bed formation (H_{pa}/H_s). The response has been used to develop an empirical model that correlates the response of semi-fluidized bed with operating variables using a second-degree polynomial equation (Eq. (3)).

$$Y = b_0' + \sum_{i=1}^{n} b_i X_i + \sum_{i=1}^{n} b_{ii} X_i^2 + \sum_{i=1}^{n}\sum_{j>1}^{n} b_{ij} X_i X_j \quad (3)$$

where Y is the predicted response, b_0', the constant coefficient, b_i, the linear coefficients, b_{ij}, the interaction coefficients, b_{ii}, the quadratic coefficients and X_i, and X_j are the coded values of the operating variables. The complete experimental range and levels of independent variables are given in Table 2. The design of this experiment is given in Table 3 (dimensional analysis) and Table 4 (statistical analysis). The number of tests required for the CCD includes the standard 2^n factorial with its origin at the center, 2n points fixed axially

Table 2. Level of independent variables

Variables	Symbol	−1	0	+1
Density (ρ_{sav}/ρ_l)	A	2.1	2.45	2.8
Particle diameter (d_{pav}/D_c)	B	28.07	28.6	29.17
Superficial gas velocity (U_{sfg}/U_{mf})	C	0.64	.80	0.97
Superficial liquid velocity (U_{sfl}/U_{mf})	D	5	6	7
Bed expansion ratio (R)	E	2	2.5	3

Table 3. Experimantal design matrix and responses (dimensional analysis)

S1 No	Density (ρ_{sav}/ρ_l)	Particle diameter (d_{pav}/D_c)	Superficial gas velocity (U_{sfg}/U_{mg})	Superficial liquid velocity (U_{sfl}/U_{mf})	Restaint positio (R)	$\Delta P_{sf}/\Delta P_{mf}$		H_{pa}/H_s	
						Cal.	Expt.	Cal.	Expt.
1	2.45	0.034942	0.670098	4.160784	2	16.932	16	0.681215	0.6375
2	2.45	0.034942	0.670098	4.160784	2.5	11.336	11	0.29614	0.4
3	2.45	0.034942	0.670098	4.160784	3	8.167	7.333	0.242833	0.225
4	2.45	0.034942	0.670098	4.160784	3.5	6.190	4.333	0.164057	0.0875
5	2.45	0.034942	0.670098	1.664314	2.5	3.311	2	0.106571	0.1
6	2.45	0.034942	0.670098	2.496471	2.5	5.708	4.333	0.188385	0.225
7	2.45	0.034942	0.670098	3.328627	2.5	8.400	6	0.282219	0.35
8	2.45	0.034942	0.670098	4.160784	2.5	11.336	8	0.38614	0.4375
9	2.45	0.034942	0.670098	4.992941	2.5	14.481	9.333	0.498878	0.55
10	2.45	0.034942	0.670098	5.825098	2.5	17.812	11.333	0.619519	0.625
11	2.45	0.034942	0.670098	6.657255	2.5	21.310	13.333	0.747366	0.775
12	245	0.034942	0.402059	4.160784	2.5	1.684	1.666	0.073033	0.0625
13	2.45	0.034942	0.536078	4.160784	2.5	4.929	3.333	0.18656	0.1375
14	2.45	0.034942	0.670098	4.160784	2.5	11.336	12.333	0.38614	0.525
15	2.45	0.034942	0.804118	4.160784	2.5	22.385	21.666	0.699642	0.725
16	2.45	0.03365	0.670098	4.160784	2.5	13.811	16.666	0.452582	0.7125
17	2.45	0.034284	0.670098	4.160784	2.5	12.524	14.754	0.418347	0.675
18	2.45	0.034942	0.670098	4.160784	2.5	11.336	13.225	0.38614	0.6
19	2.45	0.035628	0.670098	4.160784	2.5	10.237	12.063	0.355765	0.55
20	2.45	0.036338	0.670098	4.160784	2.5	9.231	11.25	0.327379	0.525
21	1.6	0.034942	0.670098	4.160784	2.5	60.337	60	0.923707	0.975
22	2.1	0.034942	0.670098	4.160784	2.5	20.757	22.5	0.529401	0.625
23	2.45	0.034942	0.670098	4.160784	2.5	11.336	12.666	0.38614	0.4375
24	2.8	0.034942	0.670098	4.160784	2.5	6.712	6.25	0.293789	0.3125
25	3.3	0.034942	0.670098	4.160784	2.5	3.522	4	0.209879	0.225

Table 4. Experimental design matrix and responses for $\Delta P_{sf}/\Delta P_{mf}$ and H_{pa}/H_s (statistical analysis)

Run	Density (ρ_{sav}/ρ_l)	Particle diameter (d_{pav}/D_c)	Superficial gas velocity (U_{sfg}/U_{mf})	Superficial liquid velocity (U_{sfl}/U_{mf})	Bed expansion ratio (R)	Expt. $\Delta P_{sf}/\Delta P_{mf}$	Expt. H_{pa}/H_s
1	2.1	0.001714	0.010936	3.328627	2	36.336	0.335
2	2.8	0.001714	0.010936	3.328627	2	11.747	0.186
3	2.1	0.001781	0.010936	3.328627	2	29.700	0.285
4	2.8	0.001781	0.010936	3.328627	2	9.602	0.158
5	2.1	0.001714	0.016404	3.328627	2	164.945	1.000
6	2.8	0.001714	0.016404	3.328627	2	53.328	0.697
7	2.1	0.001781	0.016404	3.328627	2	134.823	1.000
8	2.8	0.001781	0.016404	3.328627	2	43.589	0.893
9	2.1	0.001714	0.010936	4.992941	2	62.663	0.592
10	2.8	0.001714	0.010936	4.992941	2	20.259	0.329
11	2.1	0.001781	0.010936	4.992941	2	51.219	0.504
12	2.8	0.001781	0.010936	4.992941	2	16.559	0.279
13	2.1	0.001714	0.016404	4.992941	2	284.451	1.000
14	2.8	0.001714	0.016404	4.992941	2	91.965	1.000
15	2.1	0.001781	0.016404	4.992941	2	232.505	1.000
16	2.8	0.001781	0.016404	4.992941	2	75.170	1.000
17	2.1	0.001714	0.010936	3.328627	3	17.520	0.119
18	2.8	0.001714	0.010936	3.328627	3	5.664	0.066
19	2.1	0.001781	0.010936	3.328627	3	14.321	0.102
20	2.8	0.001781	0.010936	3.328627	3	4.630	0.056
21	2.1	0.001714	0.016404	3.328627	3	79.534	0.448
22	2.8	0.001714	0.016404	3.328627	3	25.713	0.248
23	2.1	0.001781	0.016404	3.328627	3	65.009	0.381
24	2.8	0.001781	0.016404	3.328627	3	21.018	0.211
25	2.1	0.001714	0.010936	4.992941	3	30.215	0.211
26	2.8	0.001714	0.010936	4.992941	3	9.768	0.117
27	2.1	0.001781	0.010936	4.992941	3	24.697	0.179
28	2.8	0.001781	0.010936	4.992941	3	7.984	0.100
29	2.1	0.001714	0.016404	4.992941	3	137.157	0.792
30	2.8	0.001714	0.016404	4.992941	3	44.344	0.439
31	2.1	0.001781	0.016404	4.992941	3	112.110	0.673
32	2.8	0.001781	0.016404	4.992941	3	36.246	0.374
33	1.617555	0.001748	0.01367	4.160784	2.5	189.912	0.845
34	3.282445	0.001748	0.01367	4.160784	2.5	11.809	0.199
35	2.45	0.001668	0.01367	4.160784	2.5	47.581	0.440
36	2.45	0.001828	0.01367	4.160784	2.5	29.446	0.299
37	2.45	0.001748	0.007167	4.160784	2.5	3.346	0.044
38	2.45	0.001748	0.020173	4.160784	2.5	158.986	1.000
39	2.45	0.001748	0.01367	2.181571	2.5	15.630	0.146
40	2.45	0.001748	0.01367	6.139998	2.5	62.802	0.624
41	2.45	0.001748	0.01367	4.160784	1.310793	118.931	1.000
42	2.45	0.001748	0.01367	4.160784	3.689207	18.485	0.134
43	2.45	0.001748	0.01367	4.160784	2.5	37.226	0.361
44	2.45	0.001748	0.01367	4.160784	2.5	37.226	0.361
45	2.45	0.001748	0.01367	4.160784	2.5	37.226	0.361
46	2.45	0.001748	0.01367	4.160784	2.5	37.226	0.361
47	2.45	0.001748	0.01367	4.160784	2.5	37.226	0.361
48	2.45	0.001748	0.01367	4.160784	2.5	37.226	0.361
49	2.45	0.001748	0.01367	4.160784	2.5	37.226	0.361
50	2.45	0.001748	0.01367	4.160784	2.5	37.226	0.361

at a distance; say α, from the center to generate the quadratic terms, and the replicate tests at the center; where n is the number of variables. The recommended number of tests (n_c) at the center is six; however, for the present study, eight tests have been taken for better responses.

$$N=2^n+2n+n_c \quad (4)$$

Hence, the total number of tests (N) required for the five independent variables as given by Eq. (4) is 50. For statistical analysis, a statistical software package Design-Expert 6.0.8 Portable, Stat-Ease, Inc., Minneapolis, USA, has been used for regression analysis of the semi-fluidized bed responses.

RESULTS AND DISCUSSIONS

Based on the experimental investigation and data processing thereof, the hydrodynamic parameters for the semi-fluidization bed, i.e., the semi-fluidized bed pressure drop and the height of the top packed bed, have been found to be strong functions of material properties (average particle density and particle size) and system parameters (fluid velocities and bed expansion ratio). The detailed result analysis and the correlations developed are presented below.

1. Semi-fluidized Bed Pressure Drop (ΔP_{sf})

During the investigation we found that the major contribution to total bed pressure drop in a semi-fluidized bed is due to the top packed bed. Variation of bed pressure drop with superficial liquid velocity for different material density with an initial static bed height of 0.08

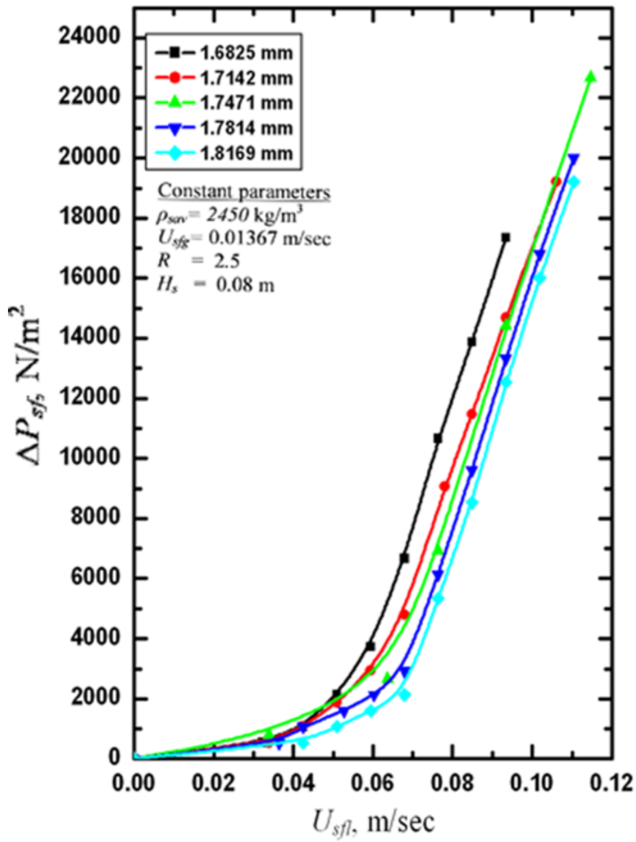

Fig. 3. Variation of ΔP_{sf} with U_{sfl} for different particle size at ρ_{sav}=2,450 kg/m^3, U_{sfg}=0.01367 m/sec and R=2.5.

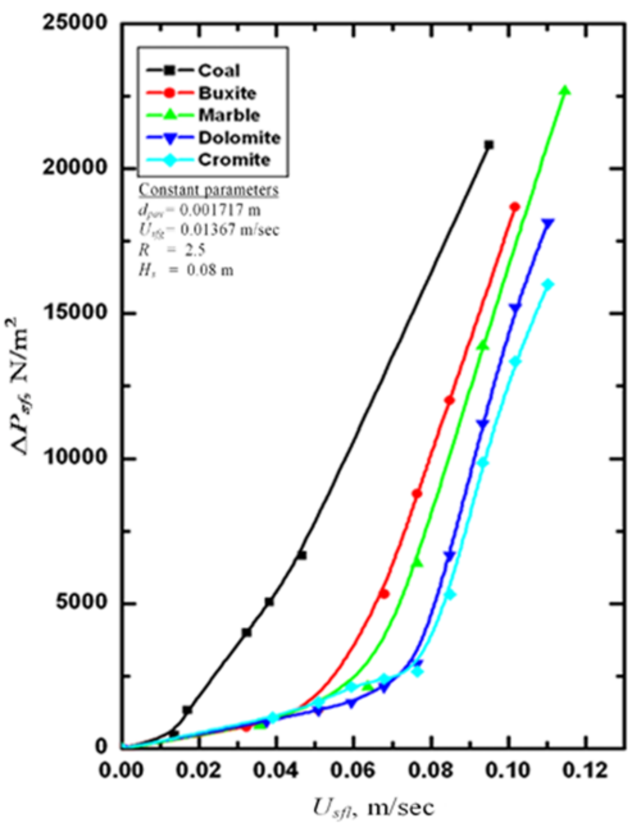

Fig. 2. Variation of ΔP_{sf} with U_{sfl} for different density material at d_{pav}=0.001717 m, U_{sfg}=0.01367 m/sec and R=2.5.

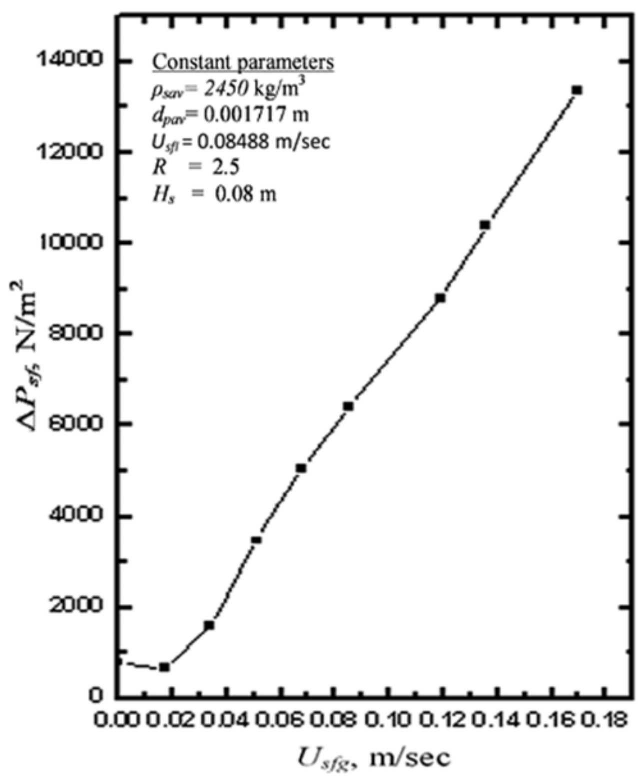

Fig. 4. Variation of ΔP_{sf} with U_{sfg} at ρ_{sav}=2,450 kg/m^3, d_{pav}=0.001717 m, U_{sfl}=0.08488 m/sec and R=2.5.

m, a mixture (70 : 30) of average particle diameter of 0.001717 m, a constant superficial air velocity of 0.01367 m/sec and a bed expansion ratio of 2.5 is shown in Fig. 2. From this, it is clearly observed that with increase in particle density the pressure drop decreases. This is because with an increase in particle density the bed weight increases, resulting in reduced transportation of materials to form a top packed bed below the top restraint, which is the main contributor for semi-fluidized bed pressure drop. Similarly, Fig. 3 presents the variation of semi-fluidized bed pressure drop with respect to superficial liquid velocities for different particle diameter (average) with an initial static bed height of 0.08 m marble particles at a constant superficial air velocity of 0.01367 m/sec and a bed expansion ratio of 2.5. As the average particle diameter increases (with the decrease of percentage of fines), the semi-fluidized bed pressure drop decreases. This is due to the presence of relatively greater number of large diameter particles in the mixture, resulting in reduced solid transportation and top packed bed formation. Pressure drop of the semi-fluidized bed increases with increase in gas velocity (Fig. 4), which is obviously due to increased material transport to the top. At low superficial gas velocity the bed pressure drop decreases, and as the superficial gas velocity increases the pressure drop increases. This is because as the superficial air velocity increases, the gas holdup in the bed increases, which in turn decreases the bed weight compared to minimum fluidization condition. The decreased weight increases the buoyancy force, thus decreasing the form drag and hence the bed pressure drop. But after a particular superficial gas velocity the bed pressure drop increases as the downward thrust imparted by the air bubble, which is because more particles are at-

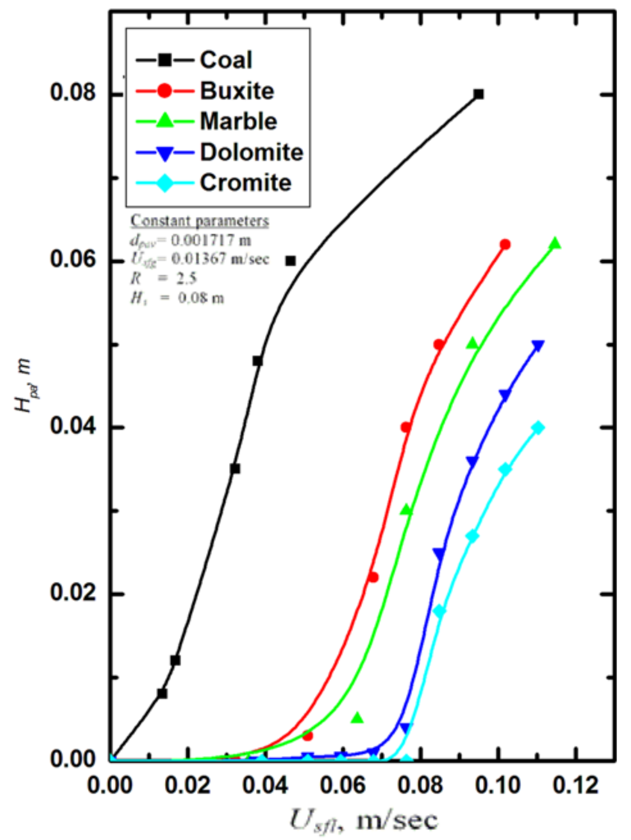

Fig. 6. Variation of H_{pa} with U_{sfl} for different density material at d_{pav}=0.001717 m, U_{sfg}=0.01367 m/sec and R=2.5.

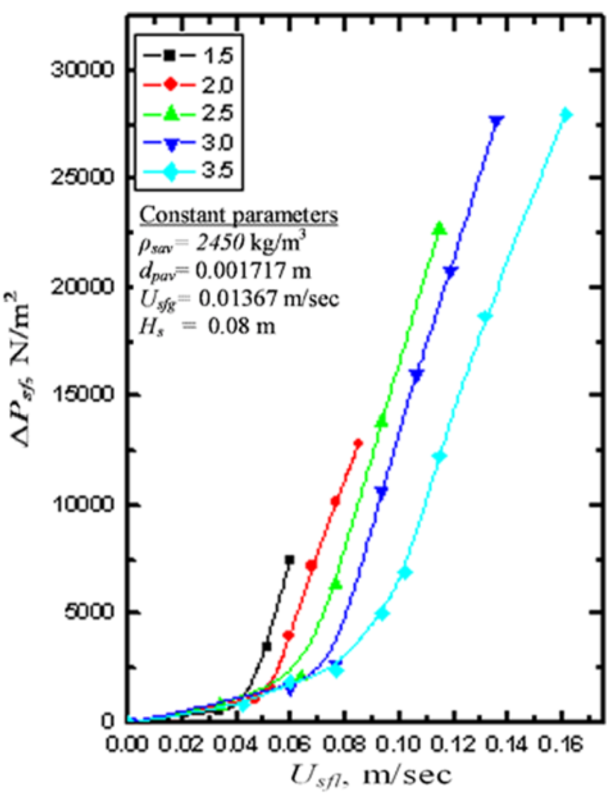

Fig. 5. Variation of ΔP_{sf} with U_{sfl} for different restraint position at ρ_{sav}=2,450 kg/m^3, d_{pav}=0.001717 m, U_{sfg}=0.01367 m/sec.

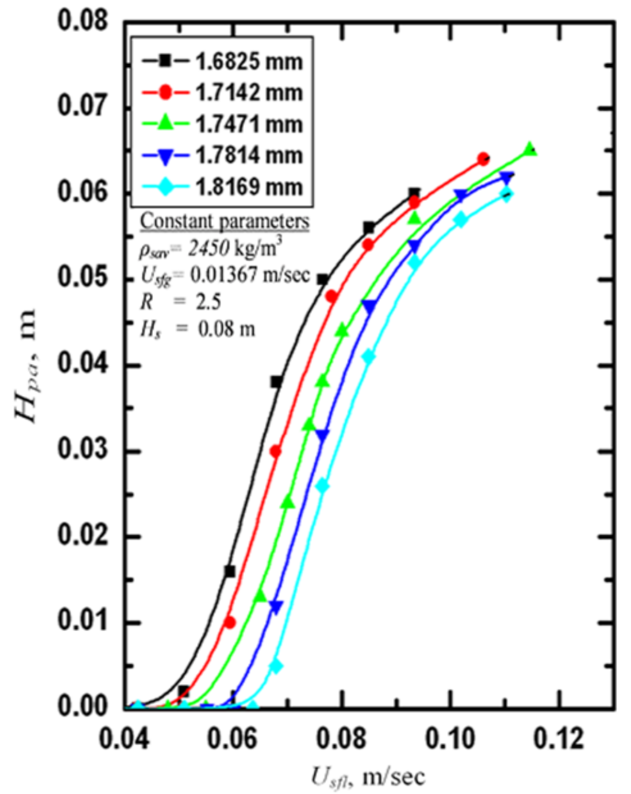

Fig. 7. Variation of H_{pa} with U_{sfl} for different particle size at ρ_{sav}= 2,450 kg/m^3, U_{sfg}=0.01367 m/sec and R=2.5.

tached to the air bubble as its size grows bigger [21]. Pressure drop of the semi-fluidized bed increases with decrease in bed expansion ratio as top packed bed formation is increased, resulting in higher semi-fluidized bed pressure drop, which is evident from Fig. 5.

2. Height of the Top Packed Bed Formation (H_{pa})

Formation of the top packed bed in a three-phase semi-fluidized bed is controlled not only by the superficial liquid velocity but also by other variables like density of solid and average particle diameter, superficial gas velocity and position of the top restraint. Fig. 6 shows variation of top packed bed formation with superficial liquid velocities for different materials with an initial static bed height of 0.08 m, a mixture (70 : 30) of average particle diameter of 0.001717 m, a constant superficial air velocity of 0.01367 m/sec and a bed expansion ratio of 2.5. For a fixed initial static bed, the weight of the bed increases with increase in density. The rate of formation of top packed, which is a result of the transportation of the bed materials to the top restraint by the liquid phase, also decreases, as is evident from Fig. 6. Decrease in average particle size of a homogeneous binary mixture is due to a relatively large fraction of fines in the mixture. The fines are transported faster to form a packed bed below the top restraint. This can be observed from Fig. 7, where a decrease in particle size has resulted in relatively higher depths of top packed bed with all other parameters remaining constant. Fig. 8 shows formation of the top packed bed with varying superficial gas velocities at a constant superficial liquid velocity of 0.08488 m/sec, a bed expansion ratio of 2.5, an initial static bed height of 0.08 m, an average particle diameter consisting of 0.001717 m marble particles of average density 2,450 kg/m^3. In this case, air as dispersed/bubble phase lifts the bed materials to the top restraint for the formation of packed bed below it. Thus the higher the superficial gas velocity, the more will be the lift of the particles, thus contributing to the increased value of the top packed bed height. Fig. 9 shows the variation of height of the top packed bed with superficial liquid velocity for different bed expansion ratio for marble particles of average particle diameter 0.001717 m, initial static bed height 0.08m and with a super-

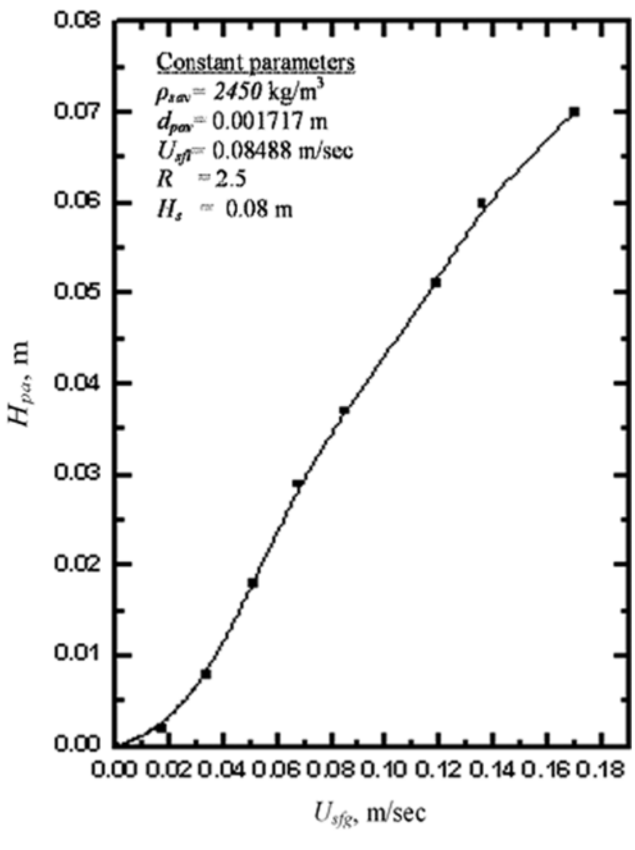

Fig. 8. Variation of H_{pa} with U_{sfg} at ρ_{sav}=2,450 kg/m^3, d_{pav}=0.001717 m, U_{sfl}=0.08488 m/sec and R=2.5.

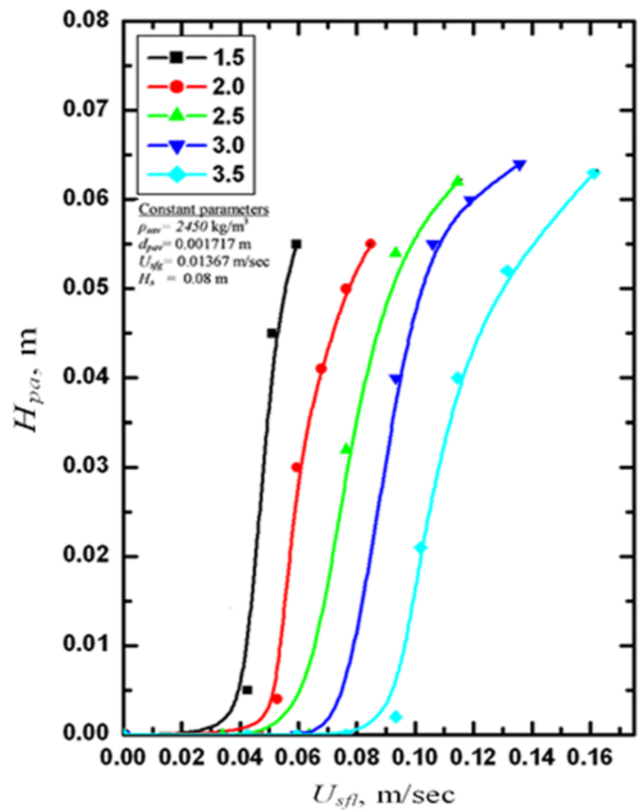

Fig. 9. Variation of H_{pa} with U_{sfl} for different restraint position at ρ_{sav}=2,450 kg/m^3, d_{pav}=0.001717 m, U_{sfg}=0.01367 m/sec.

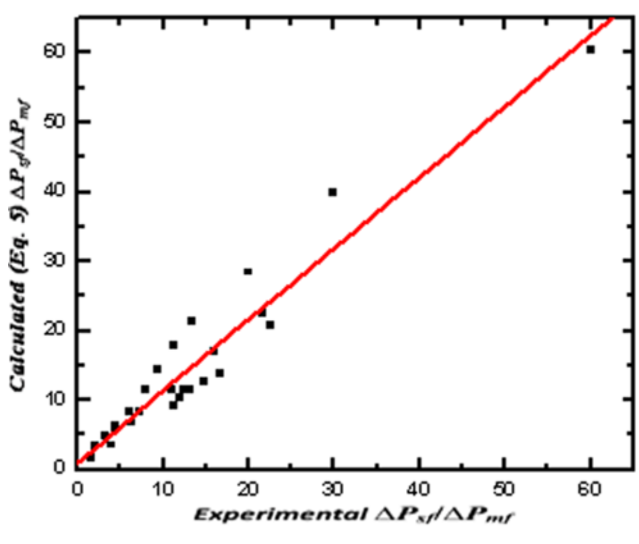

Fig. 10. Comparison between the experimental and calculated (Eq. (5)) values of $\Delta P_{sf}/\Delta P_{mf}$.

ficial gas velocity of 0.01367 m/sec. For a particular superficial liquid velocity, the closer is the position of the top restraint with respect to the initial static bed (i.e., lesser value of R), the particles are to be lifted through a shorter distance resulting in the formation of a sizeable top packed bed.

3. Development of Correlations by the Dimensional Analysis

In case of three-phase semi-fluidization, bed pressure drop and top packed bed height are found to be dependent on five operating parameters. Values of the parameters and responses for the developing correlations are given in Table 3 and the developed correlations are represented as Eqs. (5) and (6).

For dimensionless semi-fluidization pressure drop, the equation is

$$\Delta P_{sf}/\Delta P_{mf}=3\times10^{-5}(\rho_{sav}/\rho_l)^{-3.924}(d_{pav}/D_c)^{-5.243}(U_{sfg}/U_{mf})^{3.732}(U_{sfl}/U_{mf})^{1.343}R^{-1.798} \quad (5)$$

For dimensionless top packed bed height, the equation is

$$H_{pa}/H_s=9\times10^{-6}(\rho_{sav}/\rho_l)^{-2.047}(d_{pav}/D_c)^{-4.214}(U_{sfg}/U_{mf})^{3.260}(U_{sfl}/U_{mf})^{1.405}R^{-2.544} \quad (6)$$

Fig. 10 shows the comparison between the experimental and calculated values of $\Delta P_{sf}/\Delta P_{mf}$. The coefficient of correlation is found to be 0.961. Fig. 11 shows the comparison between experimental and calculated values of H_{pa}/H_s with a coefficient of correlation of 0.921.

4. Development of Correlations by the Statistical Analysis

The method of experimentation is based on statistical design of experiments (factorial design analysis) in order to bring out interaction effects of the variables, which would not otherwise be found by conventional experimentation, and to explicitly find the effect of each of the variables quantitatively on the response. In addition, the number of experiments required is far less when compared with the conventional method of data analysis and development of correlations.

The equations developed by the statistical analysis approach are:

For dimensionless semi-fluidized bed pressure drop:

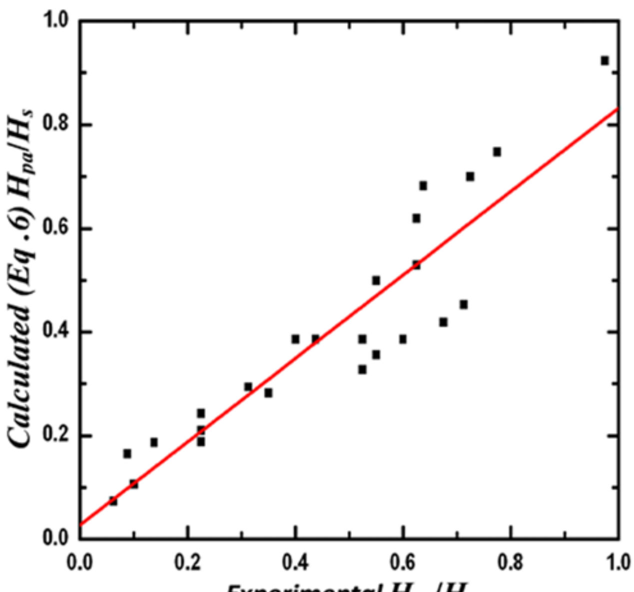

Fig. 11. Comparison of experimental and calculated (Eq. (6)) values of H_{pa}/H_s.

$$\Delta P_{sf}/\Delta P_{mf}=37.06-32.86\times A-5.53\times B+37.38\times C+14.59\times D-21.28\times E+11.10\times A^2+0.075\times B^2+7.61\times C^2-0.20\times D2+5.41\times E^2+3.14\times A\times B-19.96\times A\times C-8.31\times A\times D+10.91\times A\times E-3.92\times B\times C-1.63\times B\times D+2.14\times B\times E+10.38\times C\times D-13.64\times C\times E-5.68\times D\times E \quad (7)$$

In Fig. 12, experimental values of $\Delta P_{sf}/\Delta P_{mf}$ have been compared with calculated values obtained from (7). The value of correlation coefficient is found to be 0.974.

For dimensionless top packed bed height:

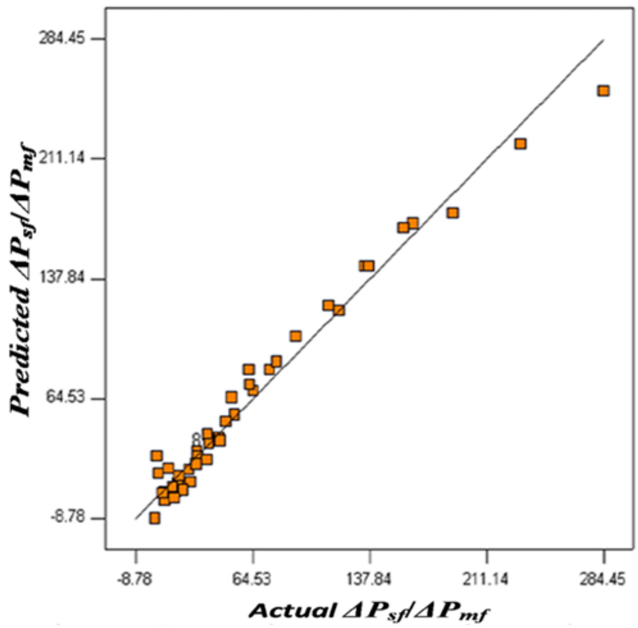

Fig. 12. Comparison of experimental and calculated (Eq. (7)) values of $\Delta P_{sf}/\Delta P_{mf}$.

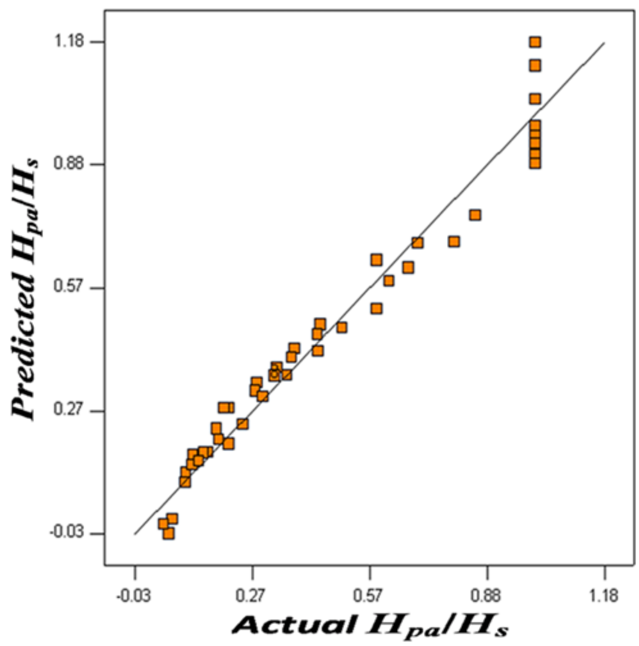

Fig. 13. Comparison of experimental and calculated (Eq. (8)) values of H_{pa}/H_s.

$$H_{pa}/H_s=0.36-0.099\times A-0.24\times B+0.22\times C+0.089\times D-0.17\times E+0.027\times A^2+5.498\times 10^{-4}\times B^2+0.027\times C^2+3.263\times 10^{-3}\times D^2+0.035\times E^2-1.936\times 10^{-3}\times A\times B-0.022\times A\times C+4.369\times 10^{-3}\times A\times D+5.652\times 10^{-3}\times A\times E-3.126\times 10^{-3}\times B\times C-1.775\times 10^{-3}\times B\times D-1.413\times 10^{-3}\times B\times E+0.022\times C\times D-0.063\times C\times E-6.613\times 10^{-3}\times D\times E \quad (8)$$

In Fig. 13, experimental values of H_{pa}/H_s have been compared with calculated values obtained from Eq. (8). The value of correlation coefficient is 0.966.

CONCLUSIONS

We studied the behavior of homogeneous binary mixtures with superficial fluid velocities in a gas-liquid-solid semi-fluidized bed with particles of different size and densities. Correlations for calculation of bed pressure drop and height top packed bed have been proposed. The values calculated from the developed correlations were compared with the experimental ones and the coefficients of correlations were found to be greater than 0.92 in each case, thus emphasizing the validity of the developed correlations over the range of the operating parameters investigated.

The present hydrodynamics study along with the correlations developed can find potential applications in unit operations and processes involving homogeneous binary mixtures of varying sizes for different materials over the present range of investigation for the design of three-phase semi-fluidized bed in which the gas phase plays an important role.

NOMENCLATURE

d : diameter [m]
G : mass velocity [$kg/m^2\cdot sec$]
H : height [m]
K, k_i : constant, (i=1, 2…10)
P : pressure [N/m^2]
R : bed expansion ratio
U : velocity [m/sec]

Greek Letters

ρ : density [kg/m^3]
Δ : difference

Subscripts

av : average
g : gas phase
l : liquid phase
mf : minimum fluidization
msf : maximum semi-fluidization
osf : onset semi-fluidization
p : particle
pa : top packed bed
s : solid/static
sf : semi-fluidization

REFERENCES

1. L. T. Fan, Y. C. Yang and C. Y. Wen, *AIChE J.*, **5**, 407 (1959).
2. L. T. Fan and C. Y. Wen, *AIChE J.*, **7**, 606 (1961).
3. G. K. Roy and K. J. R. Sarma, *J. I. Inst. Engrs., (India)*, 54 (1974).
4. G. K. Roy and H. N. Saratchandra, *Chem. Eng. J.*, **12**, 77 (1976).
5. J. Dash and G. K. Roy, *Indian Chem. J.*, 1 (1977).
6. T. C. Ho, S. J. Yau and J. R. Hopper, Department of Chemical Engineering, Lamar University, 25 (1987).
7. J. S. N. Murthy and G. K. Roy, *Indian Chem. Eng.*, **29**(2), 1 (1986).
8. J. Mydlarz, *Chem. Eng. J.*, **34**, 155 (1987).
9. K. C. Biswal, S. N. Sahoo, P. Verma, J. S. N. Murthy and G. K. Roy, *Chem. Eng. J.*, **70**, UDC 66.096.5:531.3 (1990).
10. S. H. Chern, K. Muroyama and L. S. Fan, *Chem. Eng. Sci.*, **38**, 1167 (1983).
11. S.-H. Chern, L.-S. Fan and K. Muroyama, *AIChE J.*, **30**, 288 (1984).
12. H. M. Jena, G. K. Roy and B. C. Meikap, *Indian Chem. Eng. Congress* (2006).
13. R. K. Singh, A. K. Maharathy and A. K. Mahapatra, *Chem. Eng. World*, **40**(9), 86 (2005).
14. M. Schubert and F. Larachi, *Ind. Eng. Chem. Res*., **48**(18), 8393 (2009).
15. L.-S. Fan, A. Matsuura and S.-H. Chern, *AIChE J.*, **31**, 1801 (1985).
16. S. M. M. Dias, *Extractive fermentation of ethanol by immobilized yeast cells*, *NTIS. Report*, Dept. Eng., Tech. Univ. Lisbon, Lisbon, 218 (1991).
17. S. Dehkissia, A. Baçaoui, I. Iliuta and F. Larachi, *AIChE J.*, **54**, 2120 (2008).
18. S. J. Kim, K. R. Hwang, S. Y. Cho and H. Moon, *Korean J. Chem. Eng.*, **16**, 664 (1999).
19. S. J. Kim, K. R. Hwang and S. Y. Cho, *J. Chem. Eng. Japan*, **34**, 193 (2001).
20. R. L. Is'emin, N. A. Zaitseva, A. D. Osipov and A. P. Akol'zin, *Promyshlennaya Energetika*, **2**, 37 (1995).
21. D. T. K. Dora, Y. K. Mohanty and G. K. Roy, *Chem. Eng. Sci.*, **79**, 210 (2012).